

---

# Assessment of saline-alkaline water quality and rice-crab co-culture improvement effects in the Songnen Plain

---

---

Received: 17 July 2025

---

Accepted: 28 January 2026

---

Published online: 03 February 2026

---

Cite this article as: Sun Z., Ding T., Sun C. *et al.* Assessment of saline-alkaline water quality and rice-crab co-culture improvement effects in the Songnen Plain. *Sci Rep* (2026). <https://doi.org/10.1038/s41598-026-37967-0>

Zhen Sun, Tongchao Ding, Chuang Sun, Pengcheng Gao, Yan Li, Yiming Li, Yuxing Wei, Kai Zhou, Zongli Yao & Qifang Lai

---

We are providing an unedited version of this manuscript to give early access to its findings. Before final publication, the manuscript will undergo further editing. Please note there may be errors present which affect the content, and all legal disclaimers apply.

If this paper is publishing under a Transparent Peer Review model then Peer Review reports will publish with the final article.

## **Assessment of Saline-Alkaline Water Quality and Rice-Crab Co-culture Improvement Effects in the Songnen Plain**

Zhen Sun<sup>a#</sup>, Tongchao Ding<sup>a#</sup>, Chuang Sun<sup>b</sup>, Pengcheng Gao<sup>a</sup>, Yan Li<sup>a</sup>, Yiming Li<sup>a</sup>, Yuxing Wei<sup>a</sup>, Kai Zhou<sup>a</sup>, Zongli Yao<sup>a\*</sup>, Qifang Lai<sup>a\*</sup>

a. East China Sea Fisheries Research Institute, Chinese Academy of Fisheries Sciences, 200093, Shanghai, P.R. China

b. Baicheng City Aquatic Technology Extension Station, 137099, Baicheng, P.R. China

#Co-first authors, \*Corresponding authors.

E-mail: laiqf@ecsf.ac.cn

### **Abstract**

The Songnen Plain in Northeast China is a global hotspot for soda saline-alkalization. This region suffers from severe water security challenges that limit agricultural productivity. Our assessment reveals severe irrigation hazards in the local saline-alkaline water. These waters show prevalent alkaline conditions with pH values ranging from 8.04 to 9.50. The dominant water type is  $\text{NaHCO}_3$ , with extreme sodicity levels. Importantly, 63.3% of water samples were classified as C4S4 ( $\text{EC} > 2,250 \mu\text{S cm}^{-1}$ ,  $\text{SAR} > 26$ ), indicating extreme hazard. These samples exceeded sodium hazard thresholds by 2.3-4.8 times. Hydrochemical analysis identified silicate weathering, cation exchange, and evaporative concentration as key processes driving water quality deterioration. Importantly, rice-crab

co-culture systems, particularly with juvenile crabs, effectively transform these constraints into opportunities for sustainable agriculture. The juvenile crab system achieved comprehensive improvements, reducing SAR by 41.25%, alkalinity by 1.21 mmol/L., and sodicity ( $\% \text{Na}^+ = 58.05$ ), while increasing rice yields by 10.61% and total economic output by 84.51% compared to rice monoculture. A key finding was the consistent association between crab activity and concurrent RSC increases with sodium leaching, providing a new perspective on interpreting water quality indices in integrated systems. Our findings establish rice-juvenile crab co-culture as an effective nature-based solution that simultaneously addressed water security and agricultural productivity in soda saline-alkaline regions.

## Key words

Saline-alkaline water Rice-crab co-culture, Hydrochemical assessment, Songnen Plain, Sustainable agriculture

## 1. Introduction

The Songnen Plain, situated in northeastern China ( $121^{\circ}21' \text{--} 128^{\circ}18' \text{E}$ ,  $43^{\circ}36' \text{--} 49^{\circ}26' \text{N}$ ), is a significant agricultural region that faces challenges due to saline-alkaline conditions, which adversely affect crop productivity. This region—one of the world's three major chernozem regions—is a critical national base for grain production and animal husbandry<sup>1</sup>. However, this area has become a global hotspot for soda saline-alkalization. This is constrained by soil parent material, hydrological conditions, and unsustainable anthropogenic activities (e.g., overgrazing, irrigation without drainage). The

majority of the region exhibits slight to moderate salinity levels, particularly in its central-western plains<sup>2</sup>. Despite implementing comprehensive remediation strategies-including hydraulic engineering, soil amendments, and cultivation of salt-tolerant crops-soil re-salinization remains a significant challenge<sup>3</sup>.

Rice cultivation in the Songnen Plain has emerged as an effective strategy for ameliorating saline-alkaline soils. It also enhances grain yield and sequesters organic carbon<sup>4</sup>. Field investigations revealed that integrated rice-crab co-culture systems increased crab yields by 20-40 kg/mu. This is equivalent to 500 kg/mu of annual excrement deposition. These systems also boosted economic returns by over 50% compared to monoculture rice systems. The rice-crab integrated co-culture system not only reduces soil salinity-alkalinity but also expands arable land. Furthermore, it enhances ecological resilience and restructures soil microbial communities through organic matter enrichment from aquaculture residues<sup>5</sup>. Nevertheless, the agricultural utilization of saline-alkaline water is severely limited by its complex hydrochemistry. This is characterized by elevated pH, alkalinity, salinity, and ionic imbalances.

Previous water quality assessments in this region primarily focused on pH, salinity, alkalinity, and major ion concentrations. Soda saline-alkaline waters typically exhibit high  $\text{Na}^+$  and  $\text{HCO}_3^-/\text{CO}_3^{2-}$  concentrations, as well as elevated pH<sup>1</sup>. Silicate weathering has been identified as the dominant source of  $\text{Ca}^{2+}$  and  $\text{Mg}^{2+}$  exceeding standards<sup>6</sup>. Excessive salinity and sodium adsorption ratio (SAR) exacerbate soil alkalinization, impairing crop productivity. Zhang et al.<sup>7</sup> classified surface waters into four categories based on USDA

irrigation criteria, emphasizing sodium regulation. While existing studies have extensively analyzed hydrochemical compositions, systematic evaluations of irrigation suitability for saline-alkaline water remain inadequate. Furthermore, China's recent initiatives to develop saline-alkaline lands have accelerated integrated agri-aquaculture integration utilization, such as rice-crab co-culture system. However, empirical data quantifying their benefits and constraints—particularly how aquaculture modulates pH, alkalinity, ionic loads, and irrigation water quality—are critically lacking.

This study addresses these gaps through a dual approach: (1) collecting saline-alkaline water samples from four representative zones to characterize current hydrochemical conditions, and (2) conducting comparative analyses between rice-crab co-culture and rice monoculture systems to quantify aquaculture-mediated water quality improvements. Specifically, we characterizes the hydrochemical signatures of saline-alkaline waters via multivariate statistics and geochemical modeling, develops tailored irrigation suitability indices to the Songnen Plain, and holistically evaluates the rice-crab co-culture system's efficacy in salinity mitigating alongside productivity. This integrated framework provides actionable strategies for sustainable saline-alkaline water use and soil conservation.

## 2. Materials and Methods

### 2.1 Study Area

The study area spans the western Songnen Plain in Jilin Province, China, encompassing Zhenlai County(Baicheng), Da'an

City(Baicheng), Taobei District (Baicheng), and Ulan Aodu Township (Songyuan) (Fig. 1: Remote sensing locator map). This temperate continental monsoon climate zone experiences arid to semi-arid conditions, with a mean annual temperature of 5°C and precipitation of 400-500 mm (predominantly summer rainfall). The region exhibits strong evaporation (1,200-1,600 mm/year), yielding an evaporation-to-precipitation ratio of (3-4):1. The flat topography (elevation: 120-200 m) features extensive wetlands, depressions, and interconnected lakes ("paozi" in local terminology). All water samples were collected from demonstration sites managed by the local Aquatic Technology Extension Station.

To capture representative saline-alkaline water conditions, we collected 30 surface water samples (depth: 0.2 m below water surface) from integrated agri-aquaculture integration utilization demonstration sites in Baicheng and Songyuan during Spring 2023. Samples were categorized by source/usage: source water (SW), aquaculture water (ASW), paddy field water (FW), and drainage canal water (FSW). The ASW samples represent water from aquaculture ponds with prior cultivation history, providing a baseline of historically influenced water quality. SW serves as the incoming background water, FW represents the core crop cultivation area, and FSW characterizes the final agricultural effluent. To further evaluate the impacts of aquaculture on salinity-alkalinity water dynamics, additional sampling campaigns were conducted at the Da'an demonstration site in Baicheng during the rice transplanting (May), mid-growth (August), and harvesting (September) stages in 2024. Saline-alkaline water samples were taken from three treatments, including rice monoculture, rice

juvenile crab co-culture, and rice adult crab co-culture system, with concurrent yield measurements of rice and Chinese mitten crab (*Eriocheir sinensis*).

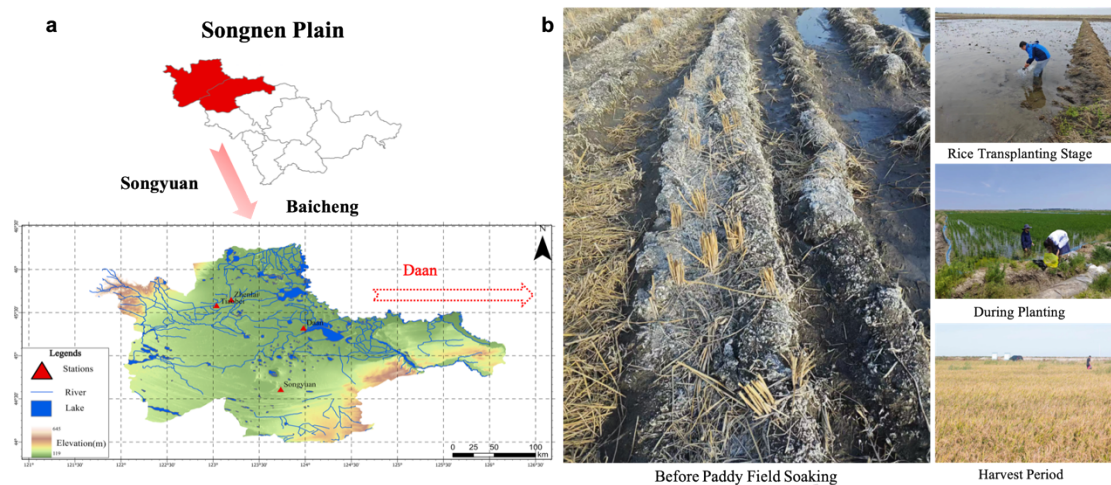


Fig. 1. Sampling locations and experimental design. a Geographical distribution of the demonstration sites within the surveyed regions. This map was created using ArcGIS Pro software (version 3.4.0; Esri Inc.) based on elevation data from the Copernicus Digital Elevation Model (CDEM, ESA) available at <https://dataspace.copernicus.eu>; b Schematic diagram of the field sampling design for a typical integrated fishery and agriculture demonstration zone.

## 2.2 Sample Collection and Analysis

Prior to sampling, 500 mL polyethylene bottles were triple-rinsed with deionized water. They were then followed by three successive rinses with ambient water. In-situ measurements of pH and salinity were obtained using calibrated portable meters (YSS ProDSS, YSI incorporated, American). Samples were immediately sealed, labeled, and transported to the laboratory under 4°C refrigeration. Cations ( $K^+$ ,  $Na^+$ ,  $Ca^{2+}$ ,  $Mg^{2+}$ ) were quantified via atomic absorption

spectrometry (GBC SavantAA, GBC instruments, Australia) following Chinese National Standard GB11904. Anions, including sulfate ( $\text{SO}_4^{2-}$ ), were measured using barium chromate spectrophotometry (HJ342). Chloride ( $\text{Cl}^-$ ) was measured by  $\text{AgNO}_3$  titration (GB11896). Carbonate species ( $\text{CO}_3^{2-}/\text{HCO}_3^-$ ) were determined by dual-indicator titration (SL83). Total dissolved solids (TDS) were determined gravimetrically at 105°C through evaporation residue method.

## 2.3 Water Quality Assessment

### (1) Ionic Balance Validation

Ion balance was used to verify the reliability of the water analysis data. The formula is as follows:

$$E (\%) = (\sum nc / \sum na) * 100$$

where E is the relative error, and nc and na represent the milliequivalent concentrations of cations and anions, respectively.

Assuming no experimental errors, the total milliequivalent concentration of anions in the water should be very close to that of cations. Theoretically, the ratio of the total milliequivalent concentration of all cations to that of all anions should be within 90%-110%. If the value of E exceeds this range, the water analysis data is considered unreliable and requires re-collection and re-measurement.

### (2) Irrigation Suitability Indices

#### Sodium Adsorption Ratio (SAR)

SAR reflects the potential of sodium to cause soil dispersion and reduce soil permeability and is an important indicator for evaluating

the suitability of water for agricultural irrigation<sup>8</sup>. The SAR is calculated as follows:

$$\text{SAR} = \text{Na}^+ / \sqrt{[\text{Ca}^{2+} + \text{Mg}^{2+}] / 2}$$

#### Sodium Percentage (%Na<sup>+</sup>)

Since the interaction of Na<sup>+</sup> with soil can reduce soil permeability, calculating the percentage of Na<sup>+</sup> is also a common method for assessing the suitability of water for agricultural irrigation<sup>9</sup>.

The %Na<sup>+</sup> is calculated as follows:

$$\% \text{Na}^+ = [\text{Na}^+ + \text{K}^+] / [\text{Ca}^{2+} + \text{Mg}^{2+} + \text{Na}^+ + \text{K}^+] \times 100$$

#### Residual Sodium Carbonate (RSC)

When the concentration of carbonate in agricultural irrigation water is higher than that of alkaline earth metals, excess carbonate will combine with Na<sup>+</sup> to form NaHCO<sub>3</sub>, affecting soil structure. Therefore, the relationship between the content of carbonate and alkaline earth metals can be calculated to assess the suitability of agricultural irrigation water. The concentration of excess carbonate is called residual sodium carbonate (RSC), which is an indicator reflecting the alkaline hazard of irrigation water<sup>8</sup>. The RSC is calculated as follows:

$$\text{RSC} = [\text{CO}_3^{2-} + \text{HCO}_3^-] - [\text{Ca}^{2+} + \text{Mg}^{2+}]$$

#### Magnesium Hazard (MH)

Szaboles and Darab proposed magnesium hazard to assess the suitability of agricultural irrigation water. Under normal circumstances, exchangeable Na<sup>+</sup> in irrigated soil can cause high levels of Mg<sup>2+</sup>. When the Mg<sup>2+</sup> content in irrigation water reaches a

certain level, magnesium alkalization may occur in the soil, affecting soil structure and producing toxic effects on crops<sup>10</sup>. The MH is calculated as follows:

$$MH = [\frac{Mg^{2+}}{Ca^{2+} + Mg^{2+}}] \times 100$$

#### Permeability Index (PI)

PI is used to measure the permeability of the soil medium<sup>10</sup>. The permeability index (PI) is a key indicator used to evaluate the suitability of irrigation water, reflecting the influence of calcium ( $Ca^{2+}$ ), magnesium ( $Mg^{2+}$ ), sodium ( $Na^+$ ), and bicarbonate ( $HCO_3^-$ ) ion concentrations on soil permeability and drainage capacity. Lower PI values usually indicate better irrigation water quality, as they suggest that the soil structure remains conducive to water movement, which is essential for healthy crop growth. Groundwater with a PI value greater than 75% is classified as Class III, indicating that it may not be suitable for irrigation, while lower PI values indicate better suitability (MDPI). The PI is calculated as follows:

$$PI = \frac{Na^+ + \sqrt{HCO_3^-}}{Ca^{2+} + Mg^{2+} + Na^+} \times 100$$

where all ion concentrations are expressed in milliequivalents per liter.

#### 2.4 Statistical Analysis

The homogeneity of variances was first assessed using Levene's test. When variances were homogeneous, standard ANOVA was applied. This was followed by Tukey's Honestly Significant Difference (HSD) post-hoc test for multiple comparisons. In cases of heterogeneous variances, Welch ANOVA and Brown-Forsythe ANOVA were used as robust corrections. For these cases, the Games-Howell method was

employed for post-hoc comparisons. The significance level was set at  $P < 0.05$  for all tests. All statistical analyses were performed using SPSS 23.0 (IBM Corp, USA, <https://www.ibm.com/products/spss-statistics>).

For geospatial and geochemical analysis, the Copernicus Digital Elevation Model (CDEM, ESA, <https://dataspace.copernicus.eu>) with a spatial resolution of 30 m was used as the data source. ArcGIS Pro software 3.4.0 (Esri Inc., USA, <https://www.esri.com/en-us/arcgis/products/arcgis-pro/overview>) was employed for terrain visualization and analysis. It was used to generate distribution maps of terrain slope and elevation. Rivers, lakes, and sampling demonstration sites were labeled in the maps (Fig. 1a). Descriptive statistics (Mean and standard deviation) were also calculated using SPSS. Origin 2022 (OriginLab Corp, USA, <https://www.originlab.com/>) was utilized to create Piper diagrams, Gibbs diagrams, ionic ratio plots, and ionic concentration boxplots. These were used for water chemistry interpretation. The US Soil Salinity Laboratory (USSL) diagram was adopted to evaluate the suitability of the saline-alkaline water for irrigation reuse.

### 3. Results

#### 3.1 Hydrochemical Characteristics of Saline-Alkaline Water Types

Descriptive statistics of four saline-alkaline water types (Aquaculture Water, ASW,  $n=8$ ; Paddy Field Water, FW,  $n=10$ ; Source Water, SW,  $n=8$ ; Drainage Canal Water, FSW,  $n=4$ ) are summarized in Table 1 and Table S1. All parameters except pH and alkalinity (mmol/L) are reported in mg/L, with cation-anion balance

error <10% confirming data reliability. Key findings include: ASW samples exhibited moderate alkalinity (pH 8.04–9.10, mean 8.74) and high salinity (TDS 1007.10–3999.31 mg/L), with mean alkalinity (11.98 mmol/L) significantly exceeding SW samples (6.72 mmol/L). FSW samples demonstrated extreme alkalinity (pH 9.02–9.50) and the highest alkalinity (18.54 mmol/L), measuring 2.76, 2.28, and 1.55 times higher than SW, FW, and ASW samples, respectively. FW samples displayed the greatest alkalinity variability (1.53–24.56 mmol/L). All water types exceeded the pH 8.5 threshold for optimal crop irrigation.

Table 1 Mean values and significance levels of hydrochemical parameters across different saline-alkaline types.

Index	ASW	SW	FW	FSW
TDS[mg/L]	2089.82 <sup>ab</sup>	659.7 <sup>b</sup>	1719.4 <sup>ab</sup>	3358.5 <sup>a</sup>
pH	8.74 <sup>ab</sup>	7.98 <sup>c</sup>	8.55 <sup>b</sup>	9.19 <sup>a</sup>
Na <sup>+</sup> [mg/L]	616.08 <sup>ab</sup>	104.95 <sup>c</sup>	415.06 <sup>b</sup>	1012.14 <sup>a</sup>
K <sup>+</sup> [mg/L]	3.70 <sup>b</sup>	3.65 <sup>b</sup>	11.85 <sup>a</sup>	14.49 <sup>a</sup>
Ca <sup>2+</sup> [mg/L]	16.70	45.57	38.82	25.73
Mg <sup>2+</sup> [mg/L]	20.75 <sup>b</sup>	16.52 <sup>b</sup>	51.92 <sup>a</sup>	45.73 <sup>a</sup>
Cl <sup>-</sup> [mg/L]	475.43 <sup>ab</sup>	30.66 <sup>b</sup>	160.87 <sup>b</sup>	873.93 <sup>a</sup>
SO <sub>4</sub> <sup>2-</sup> [mg/L]	228.21	48.87	545.68	257.20
CO <sub>3</sub> <sup>2-</sup> [mg/L]	123.01 <sup>ab</sup>	21.33 <sup>c</sup>	54.20 <sup>bc</sup>	148.60 <sup>a</sup>
HCO <sub>3</sub> <sup>-</sup> [mg/L]	605.93 <sup>ab</sup>	388.26 <sup>b</sup>	440.45 <sup>b</sup>	980.06 <sup>a</sup>

Note: Different lowercase letters (a, b, c) within the same row denote significant differences among water types at a significance level of P < 0.05. Comparisons were conducted using One-way ANOVA with Tukey's HSD test (for homogeneous variance) or Welch ANOVA with

Games-Howell post-hoc test (for heterogeneous variance). Parameters without letters indicate no significant difference ( $P > 0.05$ ).

During the sampling period in Spring 2023, although aquaculture activities for crab had not yet commenced, it is essential to acknowledge that such practices had been conducted in previous years. Consequently, the ASW samples collected during this time still reflect the hydrochemical conditions of saline-alkaline water influenced by past aquaculture. This historical context is crucial for understanding baseline conditions and the potential improvements that aquaculture could offer to saline-alkaline water quality. Furthermore, while soil return salt and alkaline were detected, this doesn't not diminish the positive effects observed from active co-culture. The significant economic benefits derived from aquaculture underscore its role in enhancing the management of saline-alkaline lands, demonstrating that the advantages of aquaculture extend beyond immediate water quality improvements to broader agricultural and economic outcomes.

Ionic Composition displayed that  $\text{HCO}_3^-$  and  $\text{Cl}^-$  were dominant anions.  $\text{Na}^+$  was the dominant cation across all types.  $\text{HCO}_3^-$  showed relative stability in ASW ( $\text{CV}=29.62\%$ ) and SW ( $\text{CV}=39.19\%$ ), while  $\text{Na}^+$  varied least in FSW ( $\text{CV}=26.36\%$ ).  $\text{SO}_4^{2-}$  exhibited extreme fluctuation in FW ( $\text{CV}=139.69\%$ ). Prior to cultivation initiation, FW samples showed elevated  $\text{SO}_4^{2-}$  release, ASW promoted  $\text{Cl}^-$  release, and FSW experienced marked increases in  $\text{Na}^+$ ,  $\text{Cl}^-$ , and alkalinity. To elucidate the distribution patterns of major ions in saline-alkaline water sources and their environmental correlations, this study

conducted a comparative analysis of concentration distributions for  $\text{Na}^+$ ,  $\text{Ca}^{2+}$ ,  $\text{Mg}^{2+}$ ,  $\text{K}^+$ ,  $\text{Cl}^-$ ,  $\text{HCO}_3^-$ ,  $\text{SO}_4^{2-}$ , and  $\text{CO}_3^{2-}$  across different saline-alkaline water types using boxplots (Fig. 2).  $\text{Cl}^-$  had universally high median concentrations (150.13 mg/L).  $\text{HCO}_3^-$  showed remarkable stability (median 458.11 mg/L).  $\text{SO}_4^{2-}$  and  $\text{CO}_3^{2-}$  exhibited high variability (medians 183.93 mg/L and 59.38 mg/L). SW ion concentrations (except  $\text{HCO}_3^-$  and  $\text{Ca}^{2+}$ ) consistently fell below saline-alkaline water medians, with  $\text{Na}^+$  and  $\text{Cl}^-$  near minimum thresholds (Fig. 2).

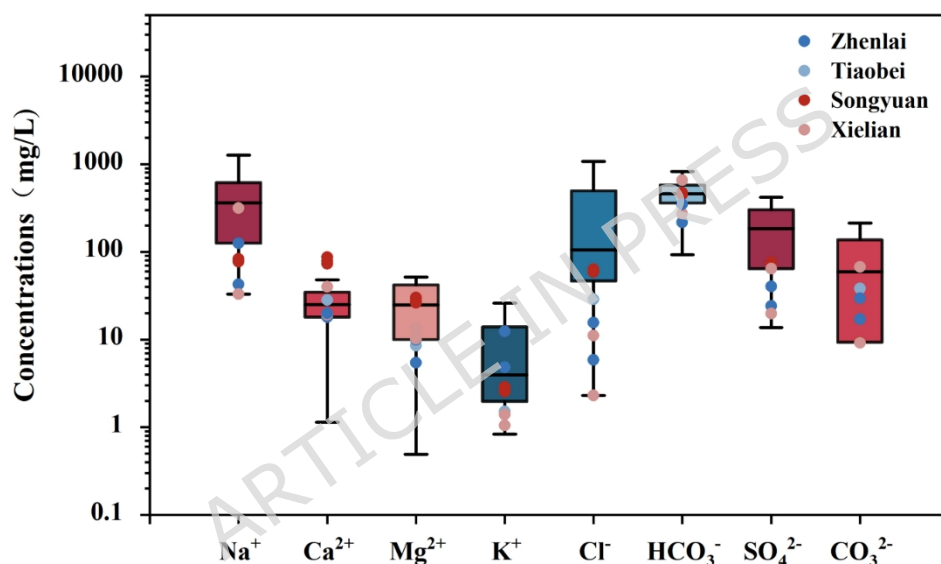
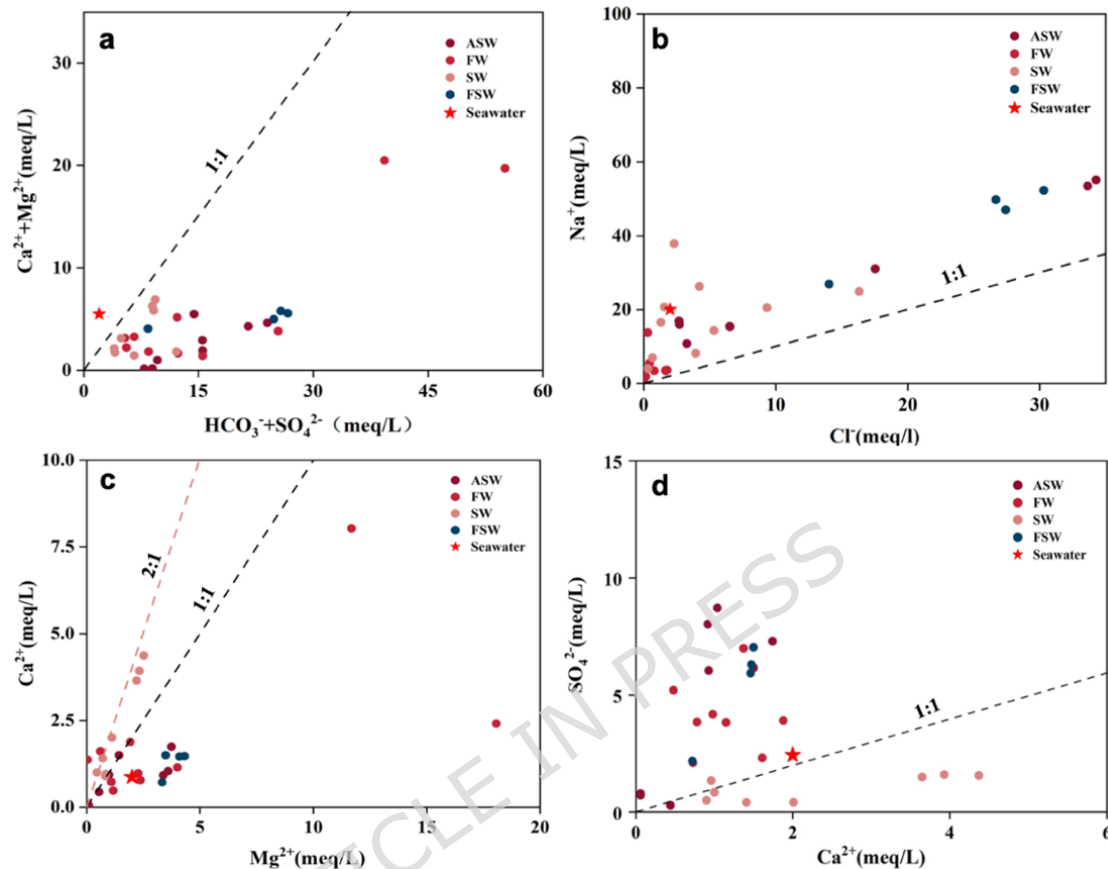


Fig 2. Boxplot comparison of major ion mass concentrations in saline-alkaline water, regional water sources, and seawater.

To elucidate hydrochemical characteristics and potential weathering sources across saline-alkaline water types, we analyzed scatterplots of  $[\text{Ca}^{2+} + \text{Mg}^{2+}]$  vs  $[\text{HCO}_3^- + \text{SO}_4^{2-}]$ ,  $[\text{Na}^+]$  vs  $[\text{Cl}^-]$ ,  $[\text{Ca}^{2+}]$  vs  $[\text{Mg}^{2+}]$ , and  $[\text{SO}_4^{2-}]$  vs  $[\text{Ca}^{2+}]$  were analyzed. Reference lines in Fig. 3a-b,d represent 1:1 equilibrium line, while Fig. 3c includes 1:1 and 2:1 equilibrium line. Artificial seawater (salinity 1.5) was prepared following Zhu Shuping's ionic formulation with eight major ions.

Scatterplot analyses revealed dominance of reverse ion exchange, carbonate/sulfate dissolution, and silicate weathering, with supplementary  $\text{Na}^+$  from silicate weathering and cation exchange



( $\text{Na}^+/\text{Cl}^-$  ratio =  $2.3 \pm 0.4$ ,  $p < 0.01$ ) (Fig. 3b).  $\text{Mg}^{2+}$  exceeded  $\text{Ca}^{2+}$  due to preferential Mg release and evaporative enrichment (Fig. 3c). Gypsum dissolution and silicate weathering primarily controlled  $\text{Ca}-\text{SO}_4$  relationships (Fig. 3d).

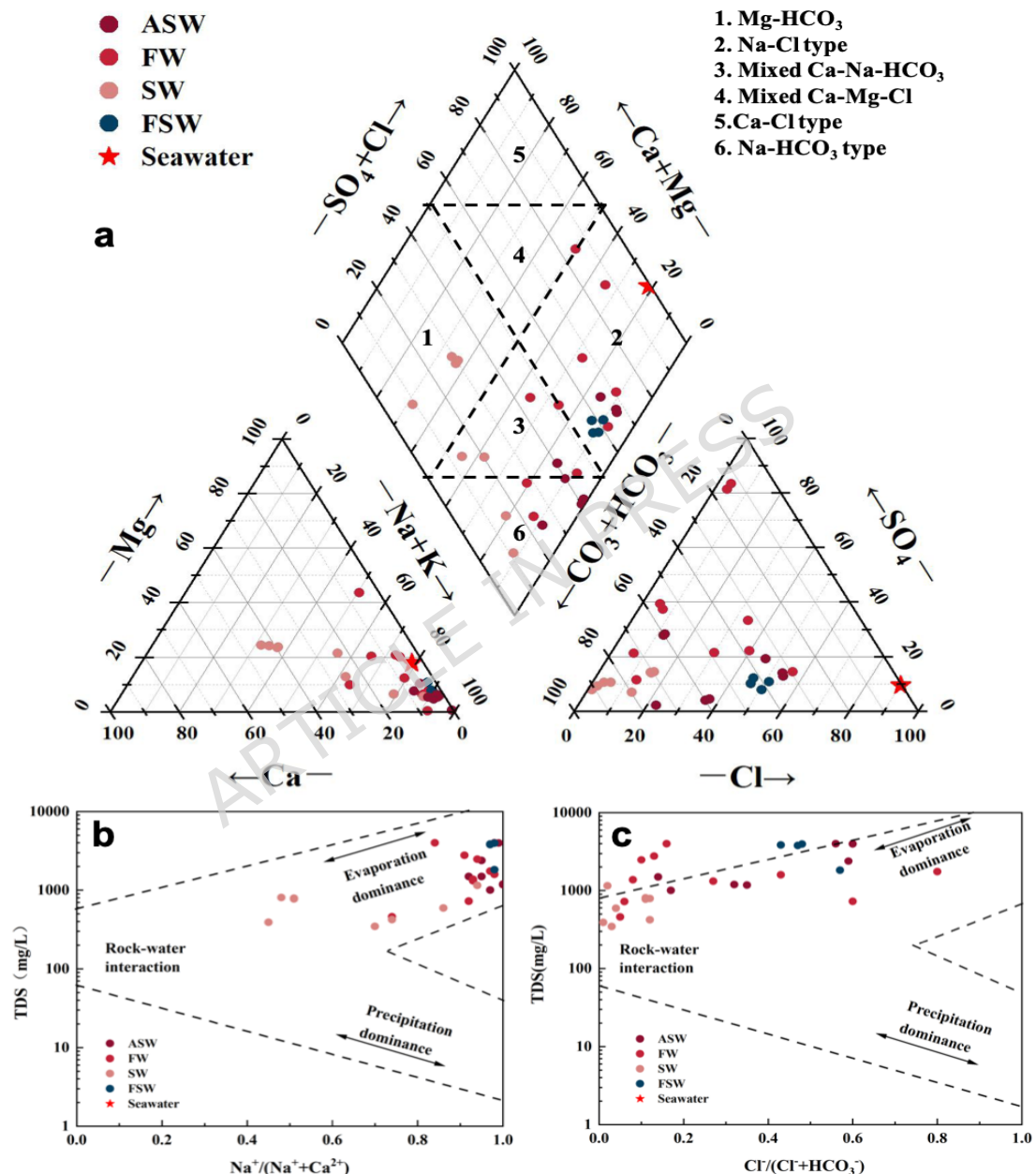
Fig.3 Ions scatter diagrams for different saline-alkaline water types. a  $[\text{Ca}^{2+} + \text{Mg}^{2+}]$  versus  $[\text{HCO}_3^- + \text{SO}_4^{2-}]$ ; b  $[\text{Na}^+]$  versus  $[\text{Cl}^-]$ ; c  $[\text{Ca}^{2+}]$  versus  $[\text{Mg}^{2+}]$ ; d  $[\text{SO}_4^{2-}]$  versus  $[\text{Ca}^{2+}]$ .

To examine the hydrochemical characteristics composition differences among various saline-alkaline water types (ASW, SW, FW, FSW, and Seawater 1.5), a Piper trilinear diagram was used (Fig. 4a).  $\text{NaHCO}_3$  was the dominant water type (60% of samples). SW samples

plotted in Zone 1 (leaching influence), while some FW, ASW, and all FSW samples plotted in Zone 2 (anthropogenic influence). ASW and artificial seawater clustered in high-Cl<sup>-</sup>/SO<sub>4</sub><sup>2-</sup>/Ca<sup>2+</sup>/Mg<sup>2+</sup> regions. Water type evolution followed: SW (HCO<sub>3</sub><sup>-</sup>-Na-Ca) → FW (HCO<sub>3</sub><sup>-</sup>-SO<sub>4</sub><sup>2-</sup>-Cl-Na) → ASW (HCO<sub>3</sub><sup>-</sup>-Cl-Na) → FSW (Na-Cl). Anthropogenic chloride enrichment (e.g., KCl fertilizers, disinfectants) drove final NaCl-type formation in populated areas. Gibbs ratio analysis (Fig. 4b-c) identified evaporation-crystallization (Na<sup>+</sup>/[Na<sup>+</sup>+Ca<sup>2+</sup>]=0.45-1)

and rock weathering ( $\text{Cl}^-/[\text{HCO}_3^- + \text{Cl}^-] = 0.01-0.99$ ) as dominant controls, with FSW showing intense evaporation signatures.

Fig.4 a the Piper diagrams of saline-alkaline water in the study area, b and c the Gibbs diagram for major processing saline-alkaline water



chemistry

### 3.2 Irrigation Suitability Assessment

Using the US salinity Laboratory (USSL) diagram (Fig. 5), we evaluated the sodium adsorption ratio (SAR) and salinity of five water types: aquaculture saline-alkaline water (ASW), source water (SW), field saline-alkaline water (FW), flowing saline-alkaline water (FSW), and artificial seawater (1.5). Only Zhenlai SW samples (C2S1: EC=412-587  $\mu$ S/cm, SAR=3.2-5.1) were suitable for most soils. Artificial seawater (1.5) and Songyuan/Daan SW samples (C3S1: EC=896-1345  $\mu$ S/cm) required salt-tolerant crops with enhanced drainage. Critically, 63.3% of the spring 2023 samples fell into the C4S4 class (EC>2250  $\mu$ S/cm, SAR>26), exceeding sodium hazard thresholds by 2.3-4.8-fold. This prevalence of extreme-hazard water in spring alone underscores the pervasive and serious nature of salinity and sodicity challenges in the region. Our data provide a conservative yet robust quantification of the baseline hazard level, against which the efficacy of management interventions (such as rice-crab co-culture) can be measured, and upon which future studies can build to explore intra-annual variability.

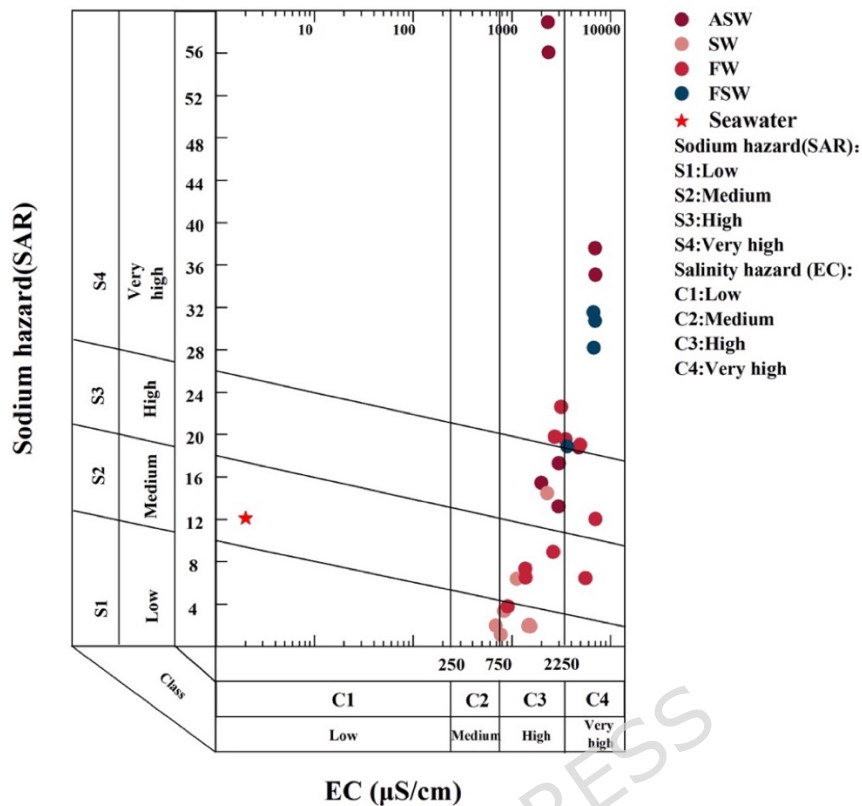


Fig.5 USSL classification of saline-alkaline water

Table 2 Evaluation results for groundwater irrigation suitability

Inde x	Criteria	Hazard description	ASW	FW	FSW	SW
			%	%	%	%
SAR	≤10	Low-sodium water, suitable	0.0	50.0	0.0	87.5
	10-18	Medium-sodium water, fairly suitable	37.5	10.0	0.0	12.5
	18-26	High-sodium water, less suitable	12.5	40.0	25.0	0.0
	>26	Extremely high sodium water, unsuitable	50.0	0.0	75.0	0.0
PI	≤25	Good water quality, suitable for irrigation	0.0	0.0	0.0	0.0
	25-75	Medium water quality, marginally suitable for irrigation	0.0	20.0	0.0	37.5

		Poor water quality, unsuitable for irrigation		100.0	80.0	100.0	62.5
Na %	≥75						
	≤20	Excellent water quality	0.0	0.0	0.0	0.0	
	20-40	Suitable water quality	0.0	0.0	0.0	50.0	
	40-60	Restricted water quality	0.0	10.0	0.0	12.5	
	60-80	Unsuitable	0.0	50.0	0.0	25.0	
RSC	>80	Extremely unsuitable	100.0	40.0	100.0	12.5	
	≤1.25	Suitable for irrigation	0.0	40.0	0.0	25.0	
	1.25- 2.50	Marginally suitable for irrigation	0.0	0.0	0.0	37.5	
	>2.5	Unsuitable for irrigation	100.0	60.0	100.0	37.5	
MH	≤30%	Suitable for irrigation	0.0	20.0	0.0	0.0	
	30-50%	Moderate risk	12.5	0.0	0.0	100.0	
	>50%	High risk	87.5	80.0	100.0	0.0	

To further explore the agricultural irrigation suitability of different saline-alkaline water, this study analyzed five indicators: SAR, permeability index (PI), sodium percentage (%Na<sup>+</sup>), residual sodium carbonate (RSC), and magnesium hazard (MH) for aquaculture water (ASW), paddy field water (FW), drainage alkali channel water (FSW), and source water (SW)(Table 2). ASW samples performed poorly across all indices (SAR: 50.0% extreme hazard; PI, %Na<sup>+</sup>, and RSC: 100.0% unsuitable; MH: 87.5% high risk). FSW samples demonstrated catastrophic unsuitability (75-100% hazard rates). FW samples showed contradictory characteristics in SAR and %Na<sup>+</sup> (50% suitability and 90% unsuitable, respectively), while other indicators were generally poor. SW samples presented partial viability (SAR/%Na<sup>+</sup>: 87.5%/50% suitable) but limitations in PI (62.5% unsuitable) and MH (100% moderate risk).

### 3.3 Impact of Rice-Crab Co-culture on Saline-alkaline Water

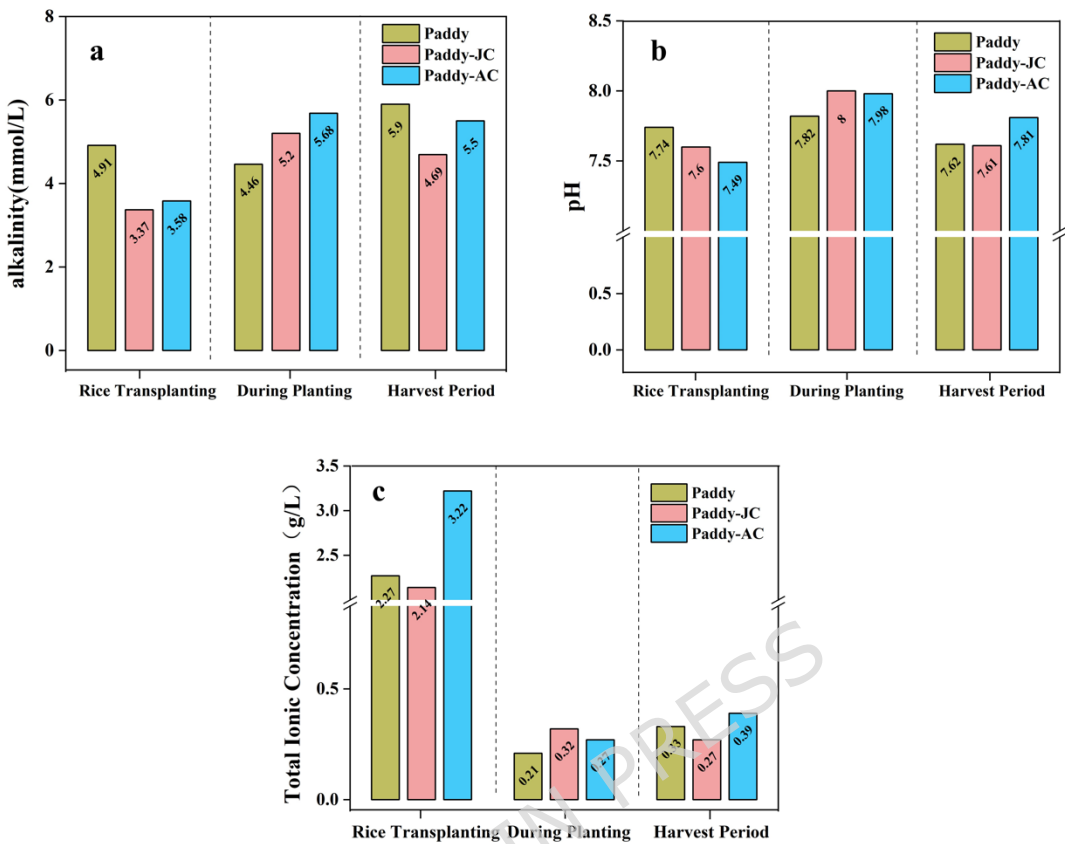


Fig.6 Changes in saline-alkaline water properties of alkalinity, pH, and Total ionic concentration under different growth stages and improvement modes.

To validate the effects of rice-crab co-culture systems on saline-alkaline water chemistry, we analyzed alkalinity, pH, and total ion content (TIC) across cultivation phases (Fig. 6). During rice transplanting, Paddy monoculture (Paddy) had peak alkalinity (4.91 mmol/L), while Rice-Juvenile Crab co-culture (Paddy-JC) showed the lowest (3.37 mmol/L). During mid-planting phase, Rice-Adult Crab (Paddy-AC) reached maximum alkalinity (5.68 mmol/L), surpassing Paddy by 27.3%. At the harvesting stage, Paddy maintained the highest alkalinity (5.90 mmol/L), while Paddy-JC demonstrated optimal mitigation (20.5% lower than Paddy). pH and Total Ion

Content (TIC) trends mirrored alkalinity, with Paddy consistently showing elevated values except during mid-planting. Paddy-JC consistently showed the lowest values at key stages (TIC: 0.27 vs 2.14 mg/L in Paddy at harvest; pH: 7.61 vs 7.6). The reduction in pH and alkalinity is agronomically significant because it mitigates the stress on crops sensitive to high pH, which can impair nutrient uptake and reduce yields.

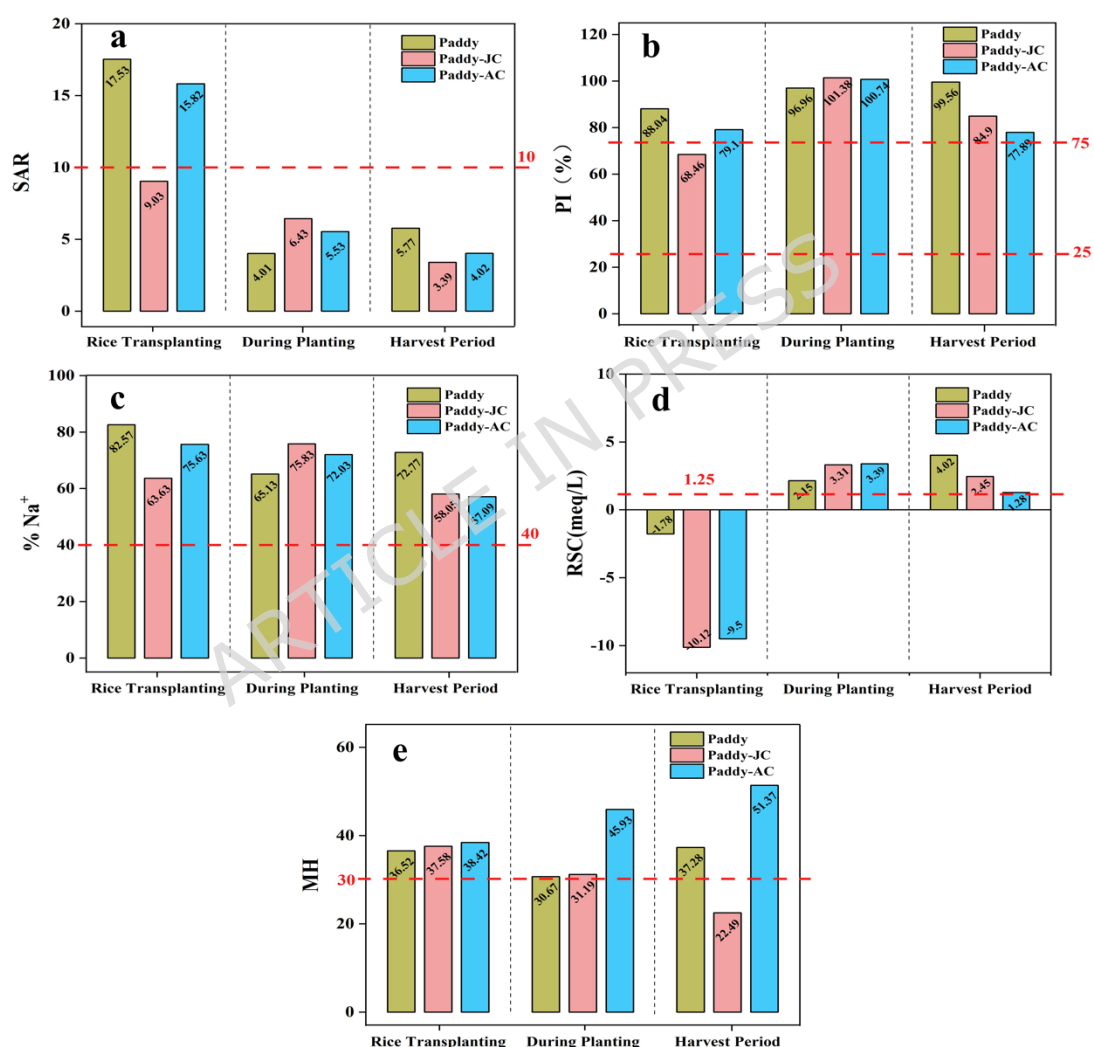


Fig.7 Changes in saline-alkaline water properties of SAR, PI, %Na<sup>+</sup>, RSC, and MH under different growth stages and improvement modes.

To investigate the impacts of Paddy-JC and Paddy-AC co-culture systems on soil physicochemical properties, we analyzed SAR, PI, %Na<sup>+</sup>, RSC, and MH across treatments (Fig. 7). At transplanting, Paddy had significantly higher SAR (17.53) than Paddy-JC (9.03) and Paddy-AC (15.82). At harvest, Paddy-AC SAR (4.02) remained lower than Paddy (5.77) but slightly higher than Paddy-JC (3.39). Paddy showed reduced permeability (PI=88.04) vs. Paddy-JC (68.46) and Paddy-AC (79.10) at transplanting, this degradation worsened in monoculture by harvest (PI=99.56), while co-culture maintained better permeability. Paddy-JC reduced %Na<sup>+</sup> by 22.9% (63.63 vs. Paddy's 82.57) at transplanting and achieved optimal balance (58.05, 20.2% lower than Paddy) at harvest. Paddy-AC demonstrated superior RSC control (1.28, 68.2% lower than Paddy). Elevated MH in Paddy-AC (51.37 vs. Paddy-JC's 22.49) correlated with juvenile crab growth. An elevated MH can disrupt the soil's calcium-magnesium balance, leading to poor soil structure and potentially toxic effects on plant root systems. Moreover, rice-crab co-culture increased rice yields by 8.73–10.61% and total economic output by 68.16–84.51% compared to rice monoculture (Table 3).

Table 3 Effects of integrated rice-crab co-culture on rice yield and *Eriocheir sinensis* biomass output.

Yield	Rice production (kg/mu)	Rice economic (RMB)	total	Crab production (kg/mu)	Crab economic (RMB)	total
Paddy	424	1272	0	0	0	
Paddy-JC	469	1407		23.5	940	
Paddy-AC	461	1383		18.9	756	

#### 4. Discussion

#### 4.1 Drivers of Saline-Alkaline Hydrochemistry and Irrigation Hazards

Our hydrochemical analysis reveals a complex interplay of natural and anthropogenic processes governing water quality in the Songnen Plain. The prevalence of  $\text{NaHCO}_3$  water types (Fig. 4a) and elevated  $\text{Na}^+/\text{Cl}^-$  ratios (Fig. 3b) strongly support silicate weathering and cation exchange as primary ion sources<sup>11</sup>, a regime intensified by evaporative concentration (Fig. 4b-c, FSW extremes). This signature is characteristic of soda saline-alkaline environments globally, consistent with recent characterizations in other endorheic basins<sup>1,11-13</sup>. Furthermore, the observed enrichment of  $\text{Mg}^{2+}$  over  $\text{Ca}^{2+}$  (Fig. 3c) aligns with the findings of Bian et al.<sup>1</sup>, which underscores the role of evaporative concentration in the region. The evolution towards Na-Cl type in drainage water (FSW) (Fig. 4a), coupled with anomalous  $\text{Cl}^-$  enrichment (Fig. 4), clearly implicates significant anthropogenic inputs—such as from KCl fertilizers and disinfectants<sup>14-15</sup>—that are overriding natural weathering controls.

The predominance of C4S4 water classification in our foundational spring 2023 (Fig. 5) coupled with widespread unsuitability across irrigation indices (Table 2), confirms the prevalence of extreme sodicity and salinity risks. Elevated SAR values ( $>26$ ) indicate that irrigation with this water will promote soil particle dispersion, severely reducing water infiltration and soil aeration, which can physically constrain root development and exacerbate water stress in crops. This finding aligns with Bian et al.'s<sup>1</sup> but contrasts with earlier reports of milder conditions<sup>6</sup>, underscoring the severity of the region challenge. These water quality constraints pose direct threats

to ecosystem health: high SAR degrades soil structure and reduces permeability, while extreme salinity and alkalinity disrupt microbial communities (e.g., favoring *Halomonadaceae*) and impair C/N/P metabolic functions<sup>16</sup>. The serious irrigation hazards documented in our spring baseline provide a compelling rationale for future research to quantify the potential intensification of these risks during drier "resurgence phases." Consequently, the direct agricultural use of most local water sources is ecologically unsustainable and necessitates prior remediation.

Despite the direct irrigation risks of spring aquaculture water (ASW) and drainage channel water (FSW), field investigations have found that farmers still reuse them. Although several studies have pointed out that such water types can enhance soil bacterial diversity, increase soil carbon reserves and fertility, regulate soil pH, improve soil structure, and reduce soil salinization and alkalinization<sup>17-19</sup>, but the persistent risks during saline-alkaline recurrence periods (such as evaporation concentration in the dry season) (fluctuation trends in Fig. 6) warn that sustainable management must be achieved through rice-crab symbiosis systems.

#### **4.2 Co-culture System Performance and Plausible Ecological linkages**

The rice-crab co-culture system, particularly the Paddy-JC treatment, demonstrates a consistent correlative association with the mitigation of key saline-alkaline constraints. The superior reduction in water alkalinity, pH, TIC (Fig. 6), SAR, %Na<sup>+</sup>, and RSC (Fig. 7) in Paddy-JC, particularly during critical growth stages (transplanting, harvest), highlights its efficacy. While specific mechanistic drivers

were not directly measured in this study, the observed improvements are consistent with known ecological processes reported in previous research. This improvement likely stems from multiple ecological mechanisms, including nutrient coupling, ionic regulation, and soil structuring through biological activity.

The correlative reductions in sodium-related indices (SAR, %Na<sup>+</sup>) and improvements in soil permeability (PI) align with the established concept that the presence of benthic organisms like crabs can influence soil physical properties through activities such as bioturbation<sup>20</sup>. Similarly, the nutrient data and yield increases (Table 3) are consistent with the documented role of animal excreta in providing bioavailable nutrients<sup>21-24</sup>. The modulation of the ionic environment (e.g., TIC and RSC) was particularly insightful. Compared with previous studies<sup>25-26</sup>, the observed increase in RSC from negative values to a low positive value in the co-culture system is a critical finding. A positive RSC typically indicates an alkaline hazard, which can raise soil pH and induce crop micronutrient deficiencies. However, the shift from a strongly negative baseline in our study suggests a more complex biogeochemical transformation. Crab bioturbation and respiration enhance the dissolution of soil minerals, such as carbonates (e.g., CaCO<sub>3</sub>). The dissolution process consumes H<sup>+</sup> and releases Ca<sup>2+</sup>, HCO<sub>3</sub><sup>-</sup>, and CO<sub>3</sub><sup>2-</sup> ions into the water, which would concurrently increase the RSC and water's alkalinity-buffering capacity. This newly released Ca<sup>2+</sup> could then participate in ion exchange, displacing Na<sup>+</sup> from soil colloids, which aligns with the observed reductions in SAR and %Na<sup>+</sup>. Thus, the RSC increase may not be a simple deterioration but rather a sign of an activated geochemical cycle where the release of calcium, even as it

elevates RSC, simultaneously facilitates the mobilization and leaching of sodium, leading to an overall improvement in soil structure and sodicity.

It is noteworthy that Paddy-JC was associated with more favorable outcomes in over 60% of the measured ecological indices compared to Paddy-AC (Fig. 6 and Fig. 7). This correlative pattern strongly suggests that juvenile crabs induce different or more pronounced system feedbacks. The higher surface-area-to-volume ratio and potentially greater mass-specific metabolic and activity rates of juvenile crabs lead to more intense bioturbation and a greater relative excretory load per unit biomass. This heightened biological activity would intensify mineral dissolution and ion exchange processes, explaining the stronger ameliorative effects observed in Paddy-JC.

#### **4.3 Research Value, Limitations and Future Research Directions**

This study provides robust, correlative evidence from a real-world agricultural setting, positioning rice-crab co-culture as a highly promising nature-based strategy for saline-alkaline land restoration in the Songnen Plain. By capturing the system's performance under practical field conditions, our findings establish a critical baseline and a compelling reference for its efficacy, particularly for the rice-juvenile crab (Paddy-JC) system in mitigating complex environmental stressors. The consistent trends observed—simultaneous mitigation of water and soil hazards alongside enhancements in productivity and economic returns—deliver a

powerful and holistic validation that aligns with global goals for sustainable intensification on marginal lands.

The observational nature of this research, which reflects the inherent complexities of large-scale agricultural studies, is a key source of its ecological relevance. While this approach places constraints on traditional statistical replication for establishing definitive causality, it successfully documents the integrated system's performance in a manner that highly controlled experiments cannot<sup>27-28</sup>. Therefore, this work should be regarded not as a terminal finding, but as a vital and robust real-world assessment that provides both a springboard for future mechanistic investigations and a valid reference for practical application. The strong correlations we report, most notably the novel geochemical interpretation of the RSC shift, generate concrete, testable hypotheses for the research community.

Guided by these clear trends and hypotheses, future research is to build effectively upon this work. The immediate priorities include: (1) Controlled experiments to quantify crab bioturbation and excretion impacts on carbonate dissolution and ion exchange; (2) Replicated trials to statistically validate the causal relationships suggested by our correlative patterns; and (3) Investigations into the role of the soil microbiome in mediating these processes<sup>29</sup>. The validation of these proposed mechanisms will solidify the theoretical foundation for a sustainable restoration strategy for which our study provides a robust empirical benchmark. Ultimately, this research pathway will enable the precise optimization of management practices, ensuring

that the full potential of this integrated agroecosystem can be realized for sustainable landscape restoration.

## 5. Conclusions

This study establishes the ecological unsustainability of direct irrigation with saline-alkaline waters from the Songnen Plain, where hydrochemical evolution—driven by evaporation and anthropogenic inputs—creates severe sodicity and salinity hazards (C4S4 classification in 63.3% of samples). In contrast, the rice-juvenile crab co-culture system (Paddy-JC) demonstrates a strong correlative link with multifaceted amelioration of these constraints. This system was consistently associated with reduced water alkalinity, pH, and TIC, alongside significant enhancements in soil health, as evidenced by a 41.2% decrease in SAR and a 20.2% reduction in  $\%Na^+$  at harvest.

A key insight of this research is the reinterpretation of a critical water quality parameter. The increase in RSC from negative to a low positive value under co-culture is not viewed as a simple deterioration, but as a potential signature of an activated, beneficial geochemical cycle. We propose that this shift marks crab-driven carbonate dissolution, a process that releases calcium to displace exchangeable sodium—thus providing a unified explanation for the concurrent rise in RSC and decline in sodium-related indices. The superior performance of juvenile crabs is hypothetically linked to their heightened metabolic and bioturbation activity, which may intensify this mechanism.

Consequently, the rice-juvenile crab co-culture system emerges not merely as a palliative measure, but as a potentially transformative agroecological strategy that actively redirects local biogeochemical

cycles to restore degraded land. Its implementation, supported by the future research outlined, presents a globally relevant model for achieving simultaneous ecological restoration and economic prosperity in saline-alkaline environments.

## **Data availability**

Data will be made available on request. The data used in this study can be provided by the first author (Zhen Sun). If necessary, please contact email: sunzhen@ecsf.ac.cn

## **Reference**

1. Bian, J., Nie, S.Y., Wang, R., Wan, H.L. & Liu, C.H. Hydrochemical characteristics and quality assessment of groundwater for irrigation use in central and eastern Songnen Plain, Northeast China. *Environ. Monit. Assess.* **382**, 1-16 (2018). <https://doi.org/10.1007/s10661-018-6774-4>
2. Gao, R.Z., Li, X.J., Zuo, L.J., Zou, B. & Wang, B. Unveiling soil salinity patterns in soda saline-alkali regions using Sentinel-2 and SDGSAT-1 thermal infrared data. *Remote Sens. Environ.* **322**, 114708 (2025). <https://doi.org/10.1016/j.rse.2025.114708>
3. Fu, J.H., Liu, Y.W., Liu, X.C., Guo, M.F. & Gao, J.Z. Screening of saline-alkali tolerant microorganisms and their promoting effects on rice growth under saline-alkali stress. *J. Clean. Prod.* **481**, 144176 (2024). <https://doi.org/10.1016/j.jclepro.2024.144176>
4. Xu, S.Q., Na, M., Huang, Y.J., Zhang, J. & Zhou, J.H. Changes in microbial carbon cycling functions along rice cultivation

chronosequences in saline-alkali soils. *Soil Biol. Biochem.* **202**, 109699 (2025). <https://doi.org/10.1016/j.soilbio.2024.109699>

5. Sun, Z., Yao, Z.L., Gao, P.C., Zhou, K. & Li, Y. Effects of fishery utilization on the physiochemical index and microbial community composition in saline-alkaline water. *ACS Omega* **9**, 18872-18881 (2024). <https://doi.org/10.1021/acsomega.3c08437>

6. Yan, J.H., Chen, J.S. & Zhang, W.Q. Study on the groundwater quality and its influencing factor in Songyuan City, Northeast China, using integrated hydrogeochemical method. *Sci. Total Environ.* **773**(15), 144958 (2021). <https://doi.org/10.1016/j.scitotenv.2021.144958>

7. Zhang, B., Song, X.F., Zhang, Y.H., Han, D.M. & Tang, C.Y. Hydrochemical characteristics and water quality assessment of surface water and groundwater in Songnen plain, Northeast China. *Water Res.* **46**(8), 2737-2748 (2012). <https://doi.org/10.1016/j.watres.2012.02.033>

8. Liu, B.S., Huang, L.H., Jiang, X.T., Huang, G.Z. & Yang, G. Quantitative evaluation and mechanism analysis of soil chemical factors affecting rice yield in saline-sodic paddy fields. *Sci. Total Environ.* **929**, 172584 (2024). <https://doi.org/10.1016/j.scitotenv.2024.172584>

9. Singh, A.K., Tewary, B.K. & Sinha, A. Hydrochemistry and quality assessment of groundwater in part of Noida metropolitan city, Uttar Pradesh. *J. Geol. Soc. India* **78**, 523-540 (2011). <https://doi.org/10.1007/s12594-011-0124-2>.

10. Arslan, H., Colak, M.G. The assessment of groundwater quality through the water quality and nitrate pollution indexes in northern Türkiye. *Environ. Monit. Assess.* **195**, 1257 (2023). <https://doi.org/10.1007/s10661-023-11854-x>.

11. Ismail, A.H., Shareef, M.A., Hassan, G., Alatar, F.M. Hydrochemistry and water quality of shallow groundwater in the Tikrit area of Salah Al Din Province, Iraq. *Appl. Water Sci.* **13**, 197 (2023). <https://doi.org/10.1007/s13201-023-02008-y>.

12. Sun, X.X., Wu, J.T., Jiang, L.J., Yao, J.N., & Chen, X.Y. Nutrient limitation and saline-alkaline stress primarily drive community and function shifts in protists inhabiting saline-sodic soils. *Agr. Ecosyst. Environ.* **396**, 110009 (2026). <https://doi.org/10.1016/j.agee.2025.110009>

13. E, J.F., Yang, S.Q., Zhang, W.F., Chen, X., Gu, Q.Y. Design and evaluation of abiological vertical shaft-subsurface ditch system for alkali spot improvement. *Agr. Water Manage.* **317**, 109625 (2025). <https://doi.org/10.1016/j.agwat.2025.109625>

14. Li, P.Y., Tian, R. & Liu, R. Solute geochemistry and multivariate analysis of water quality in the guohua phosphorite mine, Guizhou Province, China. *Expos. Health* **11**, 81-94 (2019). <https://doi.org/10.1007/s12403-018-0277-y>.

15. Sharma, A.R., Bordoloi, R., Paul, A., Gyanendra, Y. & Tripathi, O.P. Water quality and geochemical facie of high-altitude lakes in Tawang, Eastern Himalaya, India. *Environ. Sci. Pollut. R.* **31**, 24492-24511 (2024). <https://doi.org/10.1007/s11356-024-32712-4>.

16. Luo, S.Y., Yuan, J.B., Song, Y.Y., Ren, J.S. & Qi, J. Elevated salinity decreases microbial communities complexity and carbon, nitrogen and phosphorus metabolism in the Songnen Plain wetlands of China. *Water Res.* **276**, 123285 (2025). <https://doi.org/10.1016/j.watres.2025.123285>

17. Chen, L.J., Feng, Q., Li, C.S., Wei, Y.P. & Zhao, Y. Impacts of aquaculture wastewater irrigation on soil microbial functional diversity and community structure in arid regions. *Sci. Rep.-UK.* **7**, 11193 (2017). <https://doi.org/10.1038/s41598-017-11678-z>.

18. Xu, M.J., Sun, C.W., Du, Z.L. & Zhu, X.D. Impacts of aquaculture on the area and soil carbon stocks of mangrove: A machine learning study in China. *Sci. Total Environ.* **859**, 160173 (2023). <https://doi.org/10.1016/j.scitotenv.2022.160173>

19. Zhang, S.X., Rasool, G., Wang, S., Zhang, Y.W. & Guo, X.P. Biochar and Chlorella increase rice yield by improving saline-alkali soil physicochemical properties and regulating bacteria under aquaculture wastewater irrigation. *Chemosphere* **340**, 139850 (2023). <https://doi.org/10.1016/j.chemosphere.2023.139850>

20. Bashir, M.A., Liu, J., Geng, Y.C., Wang, H.Y. & Pan J.T. Co-culture of rice and aquatic animals: An integrated system to achieve production and environmental sustainability. *J. Clean. Prod.* **249**, 119310 (2020). <https://doi.org/10.1016/j.jclepro.2019.119310>

21. Chakraborty, S.C. & Chakraborty, S. Effect of dietary protein level on excretion of ammonia in Indian major carp, *Labeo rohita*, fingerlings. *Aquacult. Nutr.* **4**, 47-51 (1998). <https://doi.org/10.1046/j.1365-2095.1998.00049.x>

22. Guo, L., Zhao, L.F., Ye, J.L., Ji, Z.J. & Tang, J.J. Using aquatic animals as partners to increase yield and maintain soil nitrogen in the paddy ecosystems. *eLife* **11**, e73869 (2022). <https://doi.org/10.7554/eLife.73869>.

23. Gu, B., Zhang, X., Lam, S.K., Yu, Y.L. & van Grinsven, H.J.M. Cost-effective mitigation of nitrogen pollution from global croplands. *Nature*, 613, 77-84 (2023). <https://doi.org/10.1038/s41586-022-05481-8>

24. Zou, Z., Chu, K., Wang, M., Guo, S. Carbon footprint assessment and economic benefits of rice-fish/poultry co-culture in China. *J. Clean. Prod.* **527**, 146651 (2025). <https://doi.org/https://doi.org/10.1016/j.jclepro.2025.146651>.

25. Ghaznavi, S., Yazdani, S., Rafiee, H., Saleh, I. & Jalilian, A. Sustainable synergies of rice-fish-duck symbiosis: a life cycle assessment in Guilan province of Iran. *Results Eng.* **28**, 107226 (2025) <https://doi.org/10.1016/j.rineng.2025.107226>.

26. He, Y.L., Fu, B., Fang, C., Zhang, N.N. & Zheng, M.P. Decoding the gut-microbiota-muscle nexus: multi-omics integration reveals mTOR driven flesh modulation in rice-fish co-cultured common carp (*Cyprinus carpio*). *Aquaculture* **612**, 743090 (2026). <https://doi.org/10.1016/j.aquaculture.2025.743090>.

27. Soga, M. & Gaston, K.J. Extinction of experience among ecologists. *Trends Ecol. Evol.* **40**, 212-215 (2025). <https://doi.org/10.1016/j.tree.2024.12.010>

28. Zhao, Y.G., Wang, S.J., Li, Y., Liu, J. & Zhuo, Y.Q. Long-term performance of flue gas desulfurization gypsum in a large-scale

application in a saline-alkali wasteland in northwest China. *Agriculture, Ecosystems and Environment. Agr. Ecosyst. Environ.* **261**, 115-124 (2018). <https://doi.org/10.1016/j.agee.2018.01.009>

29. Hartmann, M. & Six, J. Soil structure and microbiome functions in agroecosystems. *Nat. Rev. Earth & Environ.* **4**, 4-18 (2023). <https://doi.org/10.1038/s43017-022-00366-w>

### **Acknowledgments**

We gratefully acknowledge the Shanghai Natural Science Foundation (25ZR1402585), the Central Public-interest Scientific Institution Basal Research Fund CAFS (2025XT0206) and the National Key R&D Program of China (2023YFD2401000).

### **Author contributions**

Z.S.: Conceptualization, Data curation, Formal analysis, Writing-original draft. T.C.D.: Data curation, Formal analysis, Figures and Tables, Investigation. C. S.: Sampling, Investigation, Data curation. P.C.G. : Investigation Y.L. : Investigation. Y.M.L.: Investigation. Y.X.W.: Investigation. K.Z.: Investigation. Z.L.Y.: Methodology, Supervision, Writing-review & editing. Q.F.L.: Conceptualization, Supervision, Funding acquisition.

### **Funding**

Shanghai Natural Science Foundation (25ZR1402585); the Central Public-interest Scientific Institution Basal Research Fund CAFS (2025XT0206); National Key R&D Program of China

(2023YFD2401000). We also thank our colleague Tianfei Cheng for the assistance with the preparation of Fig.1a.

**Competing interests**

The authors declare no competing interests.